2020 SCEC Proposal FINAL REPORT

Building a viscous mantle rheology model for Southern California constrained by tomography and postseismic deformation

Kaj M. Johnson, Indiana University, Department of Earth and Atmospheric Sciences

Thorsten Becker, Institute for Geophysics, University of Texas at Austin

Proposal Category: B. Integration and Theory
Science Objectives: P3.g, P1.a, P1.c

1. Summary of research

In 2019 we were funded to develop a workflow to generate high resolution, 3-D heterogeneous viscoelastic static Green's functions (GFs) for southern California displacements and stresses in response to slip on small fault patches defined by the SCEC community models (CFM, CVM, CRM). Deformation GFs are the basis for many SCEC studies including boundary element modeling, earthquake simulators, inversions of geodetic data for fault slip, block models of interseismic deformation, and studies of postseismic deformation. The objective of this 2020 grant was to continue development of the 3D viscoelastic Earth model for southern California with further testing and refinement of the model using postseismic deformation models of GPS-derived postseismic displacements following the 1999 Hector Mine, 2010 El Mayor – Cucapah, and 2019 Ridgecrest earthquakes. The viscoelastic GFs and 3D viscoelastic model contribute to the SCEC Community Rheology Model.

In the mantle, we estimate viscosities using laboratory derived (power-law) creep laws where spatial temperature variation is inferred from seismic velocity anomalies. The resulting mantle viscosities vary by orders of magnitude across California and the western US. We construct viscoelastic Green's functions using the mantle viscosity model using finite element code PyLith. To model postseismic deformation, we use boundary element approach with the pre-computed viscoelastic Green's Functions and model afterslip on the fault with a rate-strengthening friction law. Afterslip and mantle flow are fully coupled. We impose coseismic slip models derived from geodetic data for the Ridgefield, Hector Mine, and El Mayor-Cucapah earthquakes.

Major findings:
Postseismic mantle flow is evident in geodetic data throughout southern California following the Mw 7.1 2019 Ridgecrest earthquake. Best-fit models suggest a postseismic viscosity of 1–5×1017 Pa s at 60–100 km depth and steady-state viscosity lower than

average for the region. The 3D steady-state viscosity model predicts observed pattern of 20-year post-Hector Mine displacements fairly well but overpredicts displacements on the east side of the rupture.

2. Methods

2.1 Geodetic Data

We utilize GPS displacements downloaded from UNAVCO (PBO, 2019) from July 5 to October 23, giving a 110-day postseismic time series from the M 7.1 earthquake. To extract postseismic displacements, we invert the data using the following equation:

$$d(t) = a_0 + a_1 t + H(t - t_R)[a_2 + a_3 \ln(1 + (t - t_R)/t_r)] + \tau \int_0^t dW(t')$$

Where the coseismic rupture is modeled as a heavyside step function, the predicted cumulative postseismic offset is modeled as logarithmic decay, and all other signals including anthropogenic noise, common modes, and any seasonal components are modeled as Brownian motion. Here, a_0 through a_3 are arbitrary constants, H is the step function, t_R is the time of the earthquake, t_r is the characteristic postseismic decay time (0.01 years), and τ is the variance of the Brownian random walk. For each time series, we calculate uncertainties by bootstrapping.

2.2 3D Rheological Structure

We estimate a one-dimensional regional background viscosity profile in southern California from previous work in the region (Figure 1). We use this 1D model as a reference viscosity model to generate a 3D viscosity model for all of southern California using seismic velocity anomaly data available from the USArray (Schaeffer and Lebedev, 2014). First, we infer the temperature profile of southern California from seismic velocity anomalies (e.g. Rybach and Bunterbarth, 1984), then we compute viscosity using the relation given by Schmandt and Lin (2014):

$$\eta_{3D} = \eta_{1D} e^{\frac{E+PV}{nR(T+\Delta T)}}$$

where η_{1D} is our reference viscosity and spatially variable temperature anomalies, ΔT, are inferred from spatial variations in V_p and V_s.

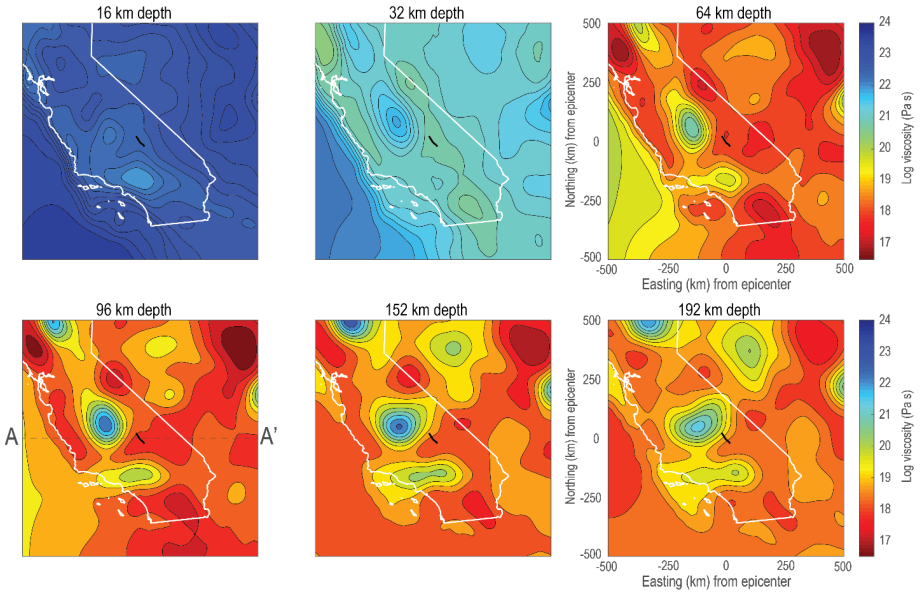

Figure 1. *Model viscosity structure. Map-view sections of 3D viscosity model at different depths*

2.4 Effective Postseismic Viscosity Formulation

To model short-term deformation, we incorporate both a Burgers rheology and a power law flow law. For our Burgers rheology, we follow the formulation of Freed et al. (2012), where local strain rate, $\dot{\varepsilon}$, decays logarithmically over time to its background value from some initial rate $\beta * \dot{\varepsilon}$ as t, the total time since a stress change, increases, with some transient relaxation time, τ:

$$\dot{\varepsilon}(t) = \dot{\varepsilon}_{\infty}[1 - e^{-\frac{t}{\tau}} + \beta e^{-\frac{t}{\tau}}]$$

The power law flow law for rocks (e.g. Carter and Tsenn, 1987) of the form.

$$\frac{\dot{\varepsilon}}{\sigma} = c\ \sigma^{n-1}$$

We compute the material parameters, c, in southern California using our viscosity model and background stress state, which is computed using the assuming some regional background strain rate. Evaluating the power law equation with these local variables, we find $c = (\eta_o {\sigma_o}^{n-1})^{-1}$. We can then generalize the power law to compute any viscosity changes in southern California with any stress changes:

$$\eta_{eff} = \eta_o \frac{{\sigma_o}^{n-1}}{{\sigma_{eff}}^{n-1}} \text{ where } \sigma_{eff} = \sigma_o + \Delta\sigma$$

We combine the power law and Burgers rheology-based viscosity formulations to get the effective postseismic viscosity:

$$\eta_{eff} = \frac{\eta_o}{\beta} \frac{{\sigma_o}^{n-1}}{(\sigma_o + \Delta\sigma_{co})^{n-1}}$$

2.5 Forward Modeling Methodology

We compute time-dependent viscoelastic Greens functions by using the numerical finite element code PyLith (Aagard et al., 2013) using a 5 by 5 km mesh out to t = 110 days after the earthquake. We use a forward-modeling technique to generate cumulative postseismic surface displacements due to coupled afterslip and viscous flow. Afterslip on the fault is modeled with a rate-strengthening friction law where shear stress on a discretized patch is a function of the normal stress, friction coefficient and rate-and-state parameters, and the instantaneous sliding velocity: $\sigma_s = \sigma_n[\mu + (a - b)\ln(v')]$.

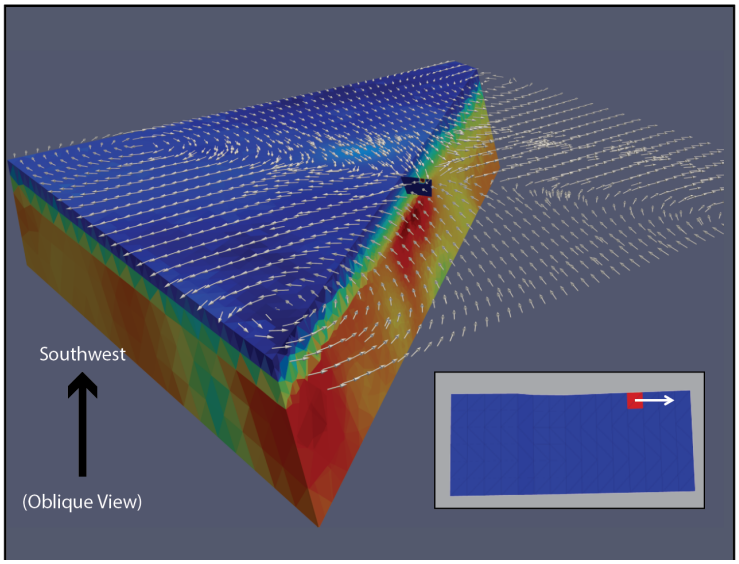

Figure 2. *Visualization of mesh shaded by viscosity. Inset figure in lower right illustrates a specific Greens function, vectors at surface show resultant cumulative deformation.*

3. Results

3.1 Ridgecrest Earthquake

We have a manuscript in revision (JGR) in which we used the steady-state mantle viscosity model illustrated in Figure 1 to compute postseismic deformation for the 2019 Ridgecrest earthquake and compare with 100-day cumulative displacements. We computed effective postseismic viscosity models from the steady-state model using power-law and Burgers contributions. We use a boundary element approach to compute coupled mantle flow and afterslip using viscoelastic Greens functions computed in PyLith. Coseismic slip is imposed on the fault (inverted from GPS and InSAR data). Afterslip rate on the fault is governed by a standard rate-strengthening friction law.

We showed that the Ridgecrest earthquake excited widespread mantle flow that is detected in geodetic data up to 400 km from the source. Figure 3 shows the fit of one of the models to the cumulative postseismic displacements (left side). We also used the inferred postseismic viscosities at depth within about 50 km radius from

the Ridgecrest hypocenter to back-calculate a range of steady-state viscosities with depth that is consistent with postseismic deformation (gray region on right side of Figure 2). This range is computed independently of the assumed 3D steady state viscosity model (Figure 1). This inferred range of steady-state (pre-earthquake) viscosities is lower than the average viscosity profile for southern California and consistent with the relatively low viscosities in our 3D steady-state model (Figure 1), providing a validation of our 2D mantle viscosity model.

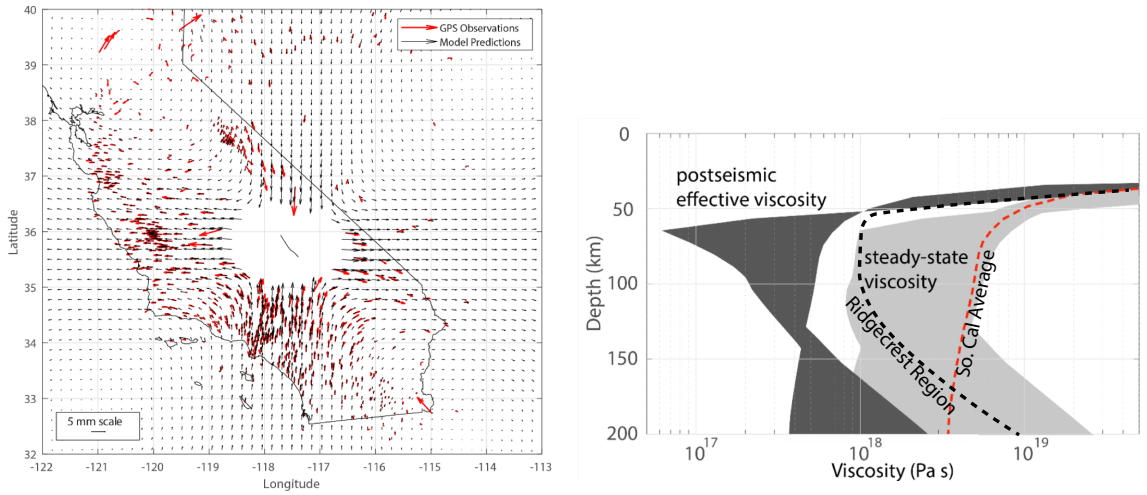

Figure 3. *Left side: Representative fit to Ridgecrest 100-day cumulative postseismic displacements for a model with effective postseismic viscosity in the range shown in previous section. Similar fit is achieved for a suite of models with steady-state strain rate (before the earthquake) of 100 nano-strain year (consistent with surface strain rate) and Burger's viscosity reduction factor of β=4-8, consistent with previous studies from other earthquakes. Right side: Range of inferred postseismic effective viscosity and steady-state viscosity (averaged within 20 km radius of epicenter). Red dashed curve is reference 1D model used to construct the 3D model.*

We also continue to test our mantle viscosity model (Figure 1) with longer-term postseismic deformation observations following the 1999 Hector Mine and 2010 El Mayor-Cucapah displacements (20-year and 10-year postseismic displacements, respectively). We use the same forward modeling technique as in the Ridgecrest modeling, however we neglect transient viscosity (power law and Burgers). Model and observed postseismic displacements are shown in Figure 4. The model matches the 20-year Hector Mine displacement field (Figure 4b) quite well to the west and south of the Eastern California Shear Zone (ECSZ), suggesting the 3D mantle viscosity model is reasonable in these areas. However, east of the ECSZ the model overpredicts displacements suggesting the relatively low model mantle viscosities (near 10^{18} Pa-s) in this region (see Figure 1) are too low and need to be refined. The 10-year El Mayor postseismic model predicts displacements (Figure 4c) that are generally larger then observed, especially to the east of the ECSZ, suggesting the model viscosities in the uppermost mantle are too low under the southern San Andreas region and east of the ECSZ. We will continue to refine the 3D mantle viscosity model to improve the model fits.

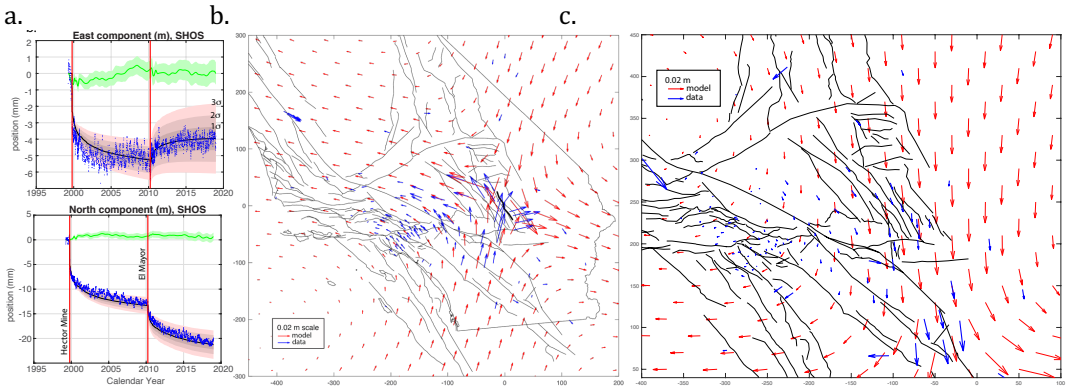

Figure 4. (a). Example time series fit for station SHOS. Blue dots are data after removing linear trend. Green curves and light green bands show mean and two standard deviation range of modeled random walk. Black curve shows mean logarithmic postseismic curve. Shades of pink show 1,2, and 3 standard deviations. (b) Cumulative 20-yr observed and modeled postseismic displacements after Hector Mine (1999-2020). (c) Cumulative 10-yr observed and modeled postseismic displacements after El Mayor-Cucapah (2010-2020).